Theor Chem Acc (2012) 131:1120
DOI 10.1007/s00214-012-1120-3

REGULAR ARTICLE

Intermolecular interactions in nitrogen-containing aromatic systems

Berkay Sütay · Adem Tekin · Mine Yurtsever

Received: 15 May 2011 / Accepted: 16 August 2011 / Published online: 4 February 2012

Abstract π–π and CH···N interactions are vital in biological systems. In this study, stacking and hydrogen-bonded interactions in pyrazine and triazine dimers were investigated by density functional theory combined with symmetry-adapted perturbation theory (DFT-SAPT) and counterpoise (CP)-corrected supermolecular MP2, SCS-MP2, B3LYP-D and CCSD(T) calculations. All interaction energies were computed using the optimized structures at the CP-corrected SCS/aug-cc-pVDZ level, which gave 1–2 kJ/mol lower interaction energies than the ones computed at the MP2 level. For both dimers, doubly hydrogen-bonded and cross-(displaced) stacked orientations were found to be the lowest energy ones. The reference CCSD(T) calculations favored the former structure in both dimer systems, whereas MP2 and SCS-MP2 located the latter as the lowest energy isomer. In particular, the former was found to be lower in energy than the latter by 2.28 and 1.01 kJ/mol at the CCSD(T)/aug-cc-pVDZ level for pyrazine and triazine, respectively. B3LYP-D produced interaction energies in agreement with the CCSD(T) at the equilibrium geometries, but it overestimates them at the short range and underestimates at the long intermonomer separations. Furthermore, it tends to give smaller equilibrium distances compared to the CCSD(T). DFT-SAPT method was in a good agreement with the reference CCSD(T) calculations. This suggests that DFT-SAPT can be employed to compute the full potential energy surface of these dimers. Moreover, DFT-SAPT calculations showed that the electrostatic and dispersion contributions are the most important energy components stabilizing these dimers. The present study aims to show which theoretical method is the most promising one for the investigation of intermolecular interactions dominated by π–π and CH···N. Therefore, the findings obtained in this study can be used to unravel the structures of nucleic acid bases and other systems stabilized by π–π and CH···N interactions.

Keywords Pyrazine · Triazine · Dimer · Intermolecular interactions · DFT-SAPT · Supermolecular calculations

Abbreviations

CP	Counterpoise
vdW	van der Waals
MP2	Second-order Møller-Plesset
SCS-MP2	Spin component-scaled second-order Møller-Plesset
CCSD(T)	Single and double excitation coupled cluster theory including perturbative triple excitations
B3LYP-D	Dispersion-corrected B3LYP
DFT	Density functional theory
IR–UV	Infrared–Ultraviolet
CBS	Complete basis set limit
SAPT	Symmetry-adapted perturbation theory
DF-DFT-SAPT	Density-fitted density functional theory combined with symmetry-adapted perturbation theory

Electronic supplementary material The online version of this article (doi:10.1007/s00214-012-1120-3) contains supplementary material, which is available to authorized users.

B. Sütay · M. Yurtsever
Chemistry Department, Istanbul Technical University, 34469 Maslak, Istanbul, Turkey

A. Tekin (✉)
Informatics Institute, Istanbul Technical University, 34469 Maslak, Istanbul, Turkey
e-mail: adem.tekin@be.itu.edu.tr

SAPT(DFT)	Density-fitted density functional theory combined with symmetry-adapted perturbation theory
HF	Hartree-Fock
PBE0AC	Asymptotically corrected PBE0 functional
LPBE0AC	Asymptotically corrected local PBE0 functional
ALDA	Adiabatic local density approximation
CMS	Center of mass
PES	Potential energy surface
PEC	Potential energy curve
PD	Parallel-displaced
IR-UV	Infrared–Ultraviolet
TOFMS	Time-of-flight mass spectroscopy
LJ	Lennard-Jones

1 Introduction

Weak intermolecular interactions in CH···X (X=O, N, π) play an important stabilizing role in many areas of chemistry and biology such as molecular recognition, enzymatic activity, crystal packing, supramolecular aggregates, DNA and spatial structure of proteins [1, 2]. Although the CH···X (X=O and N) type interactions are mostly electrostatic, the CH···π and π···π interactions are determined mostly by van der Waals (vdW) components other than the electrostatic one. Therefore, heteroaromatic molecules such as pyridine, pyrazine and triazine are good benchmark systems to study both type of interactions significant in biological systems.

The simplest system to study π···π interactions and test the efficiency of new implementations treating dispersion interactions is the benzene dimer. Huge experimental and computational efforts have been invested to explore its structures [3–25]. There are two different and nearly isoenergetic minima, tilted T-shaped and parallel-displaced (PD), for the benzene dimer. Dispersion forces are not only important for benzene, but also electrostatics as in the case of tilted T-shaped conformer. The complete basis set (CBS)-extrapolated QCISD(T) results of Janowski and Pulay [24] (dimer structures optimized at the QCISD(T)/aug-cc-pVTZ level) showed that the PD and tilted T-shaped conformers have a binding energy of 11.14 and 11.22 kJ/mol, respectively. A similar ordering was obtained by Podeszwa et al. [21] using SAPT-DFT scheme with interaction energies of 11.60 and 11.47 kJ/mol for the tilted T-shaped and PD isomers, respectively. However, CBS-extrapolated MP2 and SCS-MP2 findings gave a reverse ordering: the PD conformer is more stable than the tilted T-shaped by 4.29 and 1.62 kJ/mol at MP2 and SCS-MP2 levels, respectively [24]. Similar results were also obtained by other authors [15, 16, 22] at MP2 and SCS-MP2 levels. This is probably due to the MP2's tendency to overestimate the dispersion forces.

Recently, intermolecular interactions in pyridine dimer and trimer structures have been investigated theoretically [26, 27]. Mishra and Sathyamurthy [26] found the anti-parallel-displaced geometry as the most stable pyridine dimer geometry at the second-order Møller-Plesset, MP2/6-311++G** level. In their work, they did not optimize the dimer structures; instead they modeled different dimers by changing the monomer–monomer distances and their relative orientations. Piacenza and Grimme [27] studied the dimers and trimers of pyridine using dispersion-corrected density functional theory (DFT) method at the BLYP level of theory and calculated the interaction energies. Their results showed that the stacked and hydrogen-bonded dimers are isoenergetic and the energies of these structures were lower than the T-shaped dimer structure. For pyrazine, Mishra and Sathyamurthy [28] studied the interactions especially in stacked orientations using MP2, MP4 and single and double excitation coupled cluster theory including perturbative triple excitations [CCSD(T)]. They found the T-shaped orientation, in which the nitrogen atom is aligned toward the ring, as the most stable isomer. Among the studied dimer structures, hydrogen-bonded one was not considered. More recently, Mishra et al. [29] studied pyridine, pyrazine, triazine and tetrazine dimer structures more accurately. In particular, they optimized the stacked and hydrogen-bonded dimer structures at MP2/6-311++G(d,p) and MP2/6-311G(d,p) levels of theory, respectively. These structures employed in the CP-corrected MP2, B3LYP-D, multicoefficient extrapolated DFT (MCG3-TS) and CCSD(T) interaction energy calculations using with aug-cc-pVXZ where X = D, T and Q. They found that the hydrogen-bonded dimer structure is the most stable one for all the studied systems. Busker et al. [30] also studied the pyrazine dimers, both spectroscopically and theoretically. Their IR–UV double-resonance spectral results attributed to the existence of the hydrogen-bonded and cross-displaced stacked geometry, which was supported by the B3LYP-D/TZVP calculations and disagreed with the MP2 results, which find the T-shaped isomer as the lowest energy orientation. The difference in the calculated interaction energies that are not CP corrected was reported to be 8.2 kJ/mol.

Among the three structural isomers of triazine (1,2,3-triazine, 1,2,4-triazine and 1,2,5-triazine), 1,3,5-triazine was found to be the most stable one at spin component-scaled MP2 (SCS-MP2)/aug-cc-pVDZ level of theory. In particular, it was lower in energy than 1,2,3-and 1,2,4-triazine by 175.25 and 107.71 kJ/mol, respectively. The interaction of triazine isomers with benzene [31], water [32] and phenylacetylene [33] has already been reported.

More recently, Mishra et al. [29] studied the self-interaction in 1,3,5-triazine dimer by considering the stacked and hydrogen-bonded structures. Their MP2/CBS level calculations showed that the stacked orientations are lower in energy than the hydrogen-bonded isomer by 5.65 and 7.45 kJ/mol, respectively. However, these results were reversed at the CCSD(T)/CBS level, which finds the hydrogen-bonded isomer is more stabilized by 0.46 and 1.21 kJ/mol compared to the stacked orientations.

In this study, to address the importance of the CP correction in pyrazine dimer interaction energies and to investigate the stability of 1,3,5-triazine dimers, we have performed extensive calculations at MP2, SCS-MP2, DFT combined with symmetry-adapted perturbation theory approach in its density-fitting implementation (DF-DFT-SAPT), dispersion-corrected B3LYP-D and CCSD(T) levels of theory. We have modeled and fully optimized ten different isomers of pyrazine dimers and eight different isomers of 1,3,5-triazine dimers.

2 Computational methods

All pyrazine and 1,3,5-triazine dimer structures considered in this study have been optimized at the CP-corrected SCS-MP2 level of theory with aug-cc-pVDZ basis set using the TURBOMOLE V6.1 program package [34]. Then, these CP-corrected SCS-MP2-optimized structures have been used to compute the CP-corrected intermolecular interaction energies with supermolecular MP2, SCS-MP2 [35], B3LYP-D [36, 37] and CCSD(T) calculations using aug-cc-pVXZ basis sets with $X = \mathrm{D}$, T and in some cases Q. Furthermore, interaction energies were also calculated using symmetry-adapted perturbation theory (SAPT) [38, 39]. Since the many body version of SAPT [38] is computationally too expensive, more recently SAPT was combined with a DFT description of the monomer properties. There are two successful implementations of this combination: (1) the DFT-SAPT approach of Hasselmann and Jansen [40–43] and (2) SAPT (DFT) method of Misquitta et al. [44]. In this study, we employed the DFT-SAPT approach in its density-fitting implementation DF-DFT-SAPT [19].

The MOLPRO program package [45] was employed for all supermolecular and DF-DFT-SAPT interaction energy calculations. In the supermolecular Hartree-Fock (HF), MP2 and SCS-MP2 calculations, the density-fitting approximation was also used. In DF-HF and DF-DFT-SAPT, the cc-pV($X + 1$)Z JK-fitting basis of Weigend [46] was employed in conjunction with an aug-cc-pVXZ basis set. For the calculation of DF-MP2 and DF-SCS-MP2 correlation energies, the corresponding aug-cc-pVXZ MP2-fitting basis [47] was used.

The DFT-SAPT approach provides an understanding of the total interaction energy in terms of well-defined physically meaningful contributions: first-order electrostatics, $E_{\mathrm{el}}^{(1)}$, second-order induction, $E_{\mathrm{ind}}^{(2)}$, and dispersion, $E_{\mathrm{disp}}^{(2)}$, and the repulsive exchange corrections due to the exchange of electrons between monomers such as first-order exchange, $E_{\mathrm{exch}}^{(1)}$, second-order exchange due to induction, $E_{\mathrm{exch-ind}}^{(2)}$, and second-order exchange due to dispersion, $E_{\mathrm{exch-disp}}^{(2)}$. Moreover, effects of higher-order contributions are approximated with a $\delta(\mathrm{HF})$ term, which is the difference between the supermolecular HF energy and the sum of electrostatic, induction and their exchange counterparts obtained at the HF level. In DF-DFT-SAPT calculations, both asymptotically corrected PBE0AC [40] and LPB E0AC [19] exchange-correlation (xc) potentials in combination with the adiabatic local density approximation (ALDA) xc-kernel (to compute the response functions) were employed. Asymptotic correction required for the xc-potentials was obtained to be as the sum of experimental ionization potentials of pyrazine and triazine (9.00 and 9.80 eV, respectively) [48] and the highest occupied molecular orbital energies which were calculated to be -7.44 and -8.15 eV, respectively.

3 Results and discussion

3.1 Pyrazine dimers

As shown in Fig. 1, ten different dimer structures including hydrogen-bonded, T-shaped and stacked orientations were considered to study the intermolecular interactions in the pyrazine dimer. To discuss the effect of optimized dimer geometries in the interaction energies, we calculated the CP-corrected interaction energies at the levels of MP2, SCS-MP2, DFT-SAPT(PBE0AC), B3LYP-D and CCSD(T) employing aug-cc-pVDZ basis set in orientations **A** and **D,** which were optimized at MP2, SCS-MP2 and CP-SCS-MP2 levels using aug-cc-pVDZ basis set, respectively. The corresponding results were listed in Table 1. At all levels, interaction energies obtained for these two dimers were arranged in the following decreasing order MP2 > SCS-MP2 > CP-SCS-MP2. This result is consistent with MP2's underestimation of center of mass (cms) distances, which has already been observed for acetylene-benzene [49] and acetylene-furan [50] dimers. In particular, the cms distances were obtained to be 5.78, 5.85 and 5.87 Å for **A** orientation and 4.20, 4.30 and 4.36 Å for **D** at MP2, SCS-MP2 and CP-SCS-MP2 levels of geometry optimizations, respectively. A similar trend was also found for the other orientations of the pyrazine dimer. A notable

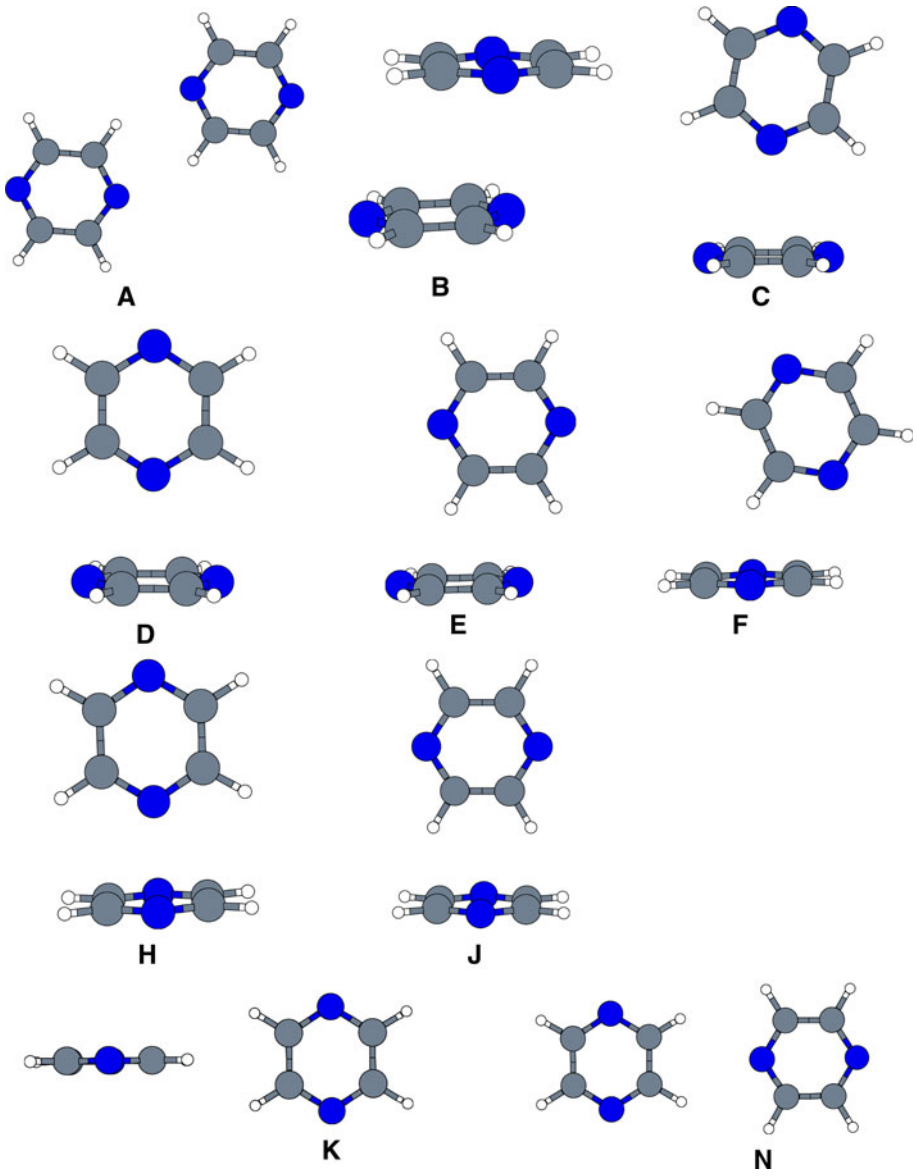

Fig. 1 Pyrazine dimer orientations considered in this study

Table 1 Calculated interaction energies (E_{int}) [in kJ/mol] at MP2, SCS-MP2, B3LYP-D, DFT-SAPT (PBE0AC) and CCSD(T) levels using aug-cc-pVDZ basis set for A and D pyrazine orientations, which have been optimized at MP2, SCS-MP2 and CP-SCS-MP2 levels employing aug-cc-pVDZ basis set

Isomer	MP2	SCS-MP2	B3LYP-D	DFT-SAPT(PBE0AC)	CCSD(T)
A[a]	−17.36	−13.52	−19.06	−12.65	−15.42
A[b]	−17.66	−14.20	−19.17	−13.40	−15.95
A[c]	−17.79	−14.52	−19.06	−13.73	−16.19
D[a]	−16.31	−8.52	−10.85	−6.13	−9.07
D[b]	−17.23	−10.53	−12.03	−8.25	−11.14
D[c]	−17.31	−11.12	−12.20	−8.94	−11.76

[a] E_{int} obtained using MP2-optimized geometries

[b] E_{int} obtained using SCS-MP2-optimized geometries

[c] E_{int} obtained using CP-SCS-MP2-optimized geometries

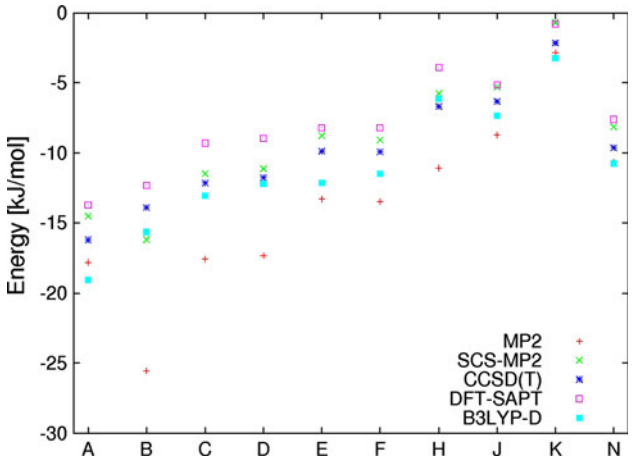

Fig. 2 Interaction energies of CP-SCS-MP2/aug-cc-pVDZ-optimized pyrazine dimers calculated at MP2, SCS-MP2, B3LYP-D, DFT-SAPT(PBE0AC) and CCSD(T) levels employing aug-cc-pVDZ basis set

difference was obtained especially when switching from MP2 to SCS-MP2 in **D** orientation, for example, at the CCSD(T) level, interaction energies differed by 2.07 kJ/mol. This difference was less dramatic in structure **A**. Moreover, interaction energies obtained using SCS-MP2 geometries were much closer to the CP-SCS-MP2 ones. These results suggest that CP-SCS-MP2-optimized geometries are the best for the intermolecular interaction energy calculations. Therefore, all the remaining pyrazine orientations were also optimized at the CP-SCS-MP2 level with aug-cc-pVDZ basis set.

Interaction energies of all pyrazine orientations shown in Fig. 1 were calculated at MP2, SCS-MP2, DFT-SAPT(PBE0AC), B3LYP-D and CCSD(T) levels with aug-cc-pVDZ basis set using CP-SCS-MP2/aug-cc-pVDZ geometries and plotted in Fig. 2 to show the performance of all theoretical methods. It is clear from Fig. 2 that in all methods except MP2 and SCS-MP2 the doubly hydrogen-bonded structure (**A** in Fig. 1) was obtained as the most stable isomer. On the other hand, MP2 and SCS-MP2 favored the cross-displaced stacked geometry (**B** in Fig. 1) in which π–π interaction is dominant. Trends observed in CCSD(T) were almost reproduced with B3LYP-D and DFT-SAPT(PBE0AC). Even though SCS-MP2 fails to locate the structure **A** as the most stable, it performs quite well for the other orientations compared to CCSD(T). As expected, MP2 overestimates the interaction energies almost for all the structures. Additionally, we also performed most of these interaction energy calculations using aug-cc-pVTZ basis set. The most time consuming CCSD(T) calculations were only carried out for the most symmetric orientations. As can be seen from Table 2, energy ordering obtained from the calculations employing the aug-cc-pVDZ is preserved in triple-zeta computations. In particular, MP2 and SCS-MP2 located **B** lower in energy than **A** by 8.83 and 2.38 kJ/mol, respectively. On the other hand, **A** found to be lower in energy than **B** in B3LYP-D, DFT-SAPT(PBE0AC) and DFT-SAPT(LPBE0AC) by 2.83, 0.41 and 0.13 kJ/mol, respectively. Although CCSD(T)/aug-cc-pVTZ calculations for **B** are not available, we expect that the 2.28 kJ/mol energy difference between **A** and **B** isomers calculated at CCSD(T)/aug-cc-pVDZ level would be the same at CCSD(T)/aug-cc-pVTZ level. Obviously, interaction energies obtained from all methods for the most stable pyrazine dimers (**A** and **B**) are much lower than the benzene dimer (11.14–11.22 kJ/mol [24] and 11.60–11.47 kJ/mol [21]). Similar to the tilted T-shaped conformer of benzene, **E** and **F** pyrazine isomers are mostly stabilized by CH$\cdots\pi$ interactions and their

Table 2 Calculated interaction energies (Eint) [in kJ/mol] at MP2, SCS-MP2, B3LYP-D, DFT-SAPT (PBE0AC), DFT-SAPT (LPBE0AC) and CCSD(T) levels using aug-cc-pVTZ basis set for all pyrazine orientations, which have been optimized at the CP-SCS-MP2 level employing aug-cc-pVDZ basis set

Isomer	E_{int}					
	MP2	SCS-MP2	B3LYP-D	DFT-SAPT (PBE0AC)	DFT-SAPT (LPBE0AC)	CCSD(T)
A	−19.15	−15.81	−19.01	−14.68	−16.57	−17.61
B	−27.98	−18.19	−16.18	−14.27	−16.44	–
C	−19.03	−12.73	−13.39	−10.88	−12.51	–
D	−18.78	−12.37	−12.53	−10.56	−12.11	−12.92
E	−14.75	−10.03	−12.34	−9.18	−10.48	–
F	−14.90	−10.28	−11.57	−8.20	−10.59	–
H	−12.16	−6.66	−6.57	−5.29	−6.43	–
J	−9.73	−6.21	−7.52	−5.14	−6.88	−7.03
K	−3.45	−1.21	−3.28	−1.33	−2.04	–
N	−11.46	−8.83	−10.75	−7.60	−9.52	–

binding energies are very close to that of benzene. Additionally, N···π interaction in pyrazine dimers (**C**, **D** and **H**) is stronger than CH···π. More specifically, for example, at the DFT-SAPT(LPBE0AC)/aug-cc-pVTZ level, **C** and **D** conformers have lower binding energies than **E** and **F** by 2.03–1,92 and 1.63–1.52 kJ/mol, respectively. Besides these different types of interactions, a side-by-side orientation in which the C–C bond of pyrazine is directed to the C–C bond of other pyrazine, **K**, was found as the least stable pyrazine isomer.

Two-color time-of-flight mass spectroscopy (two-color TOFMS) technique has been employed to determine the dimer structures of pyrazine, pyrimidine and pyrazine–pyrimidine [51, 52]. These studies have been complemented by the dimer structure elucidations based on Lennard-Jones (LJ) potential with the exception that if a hydrogen bonding interaction is possible for a pair of atoms, then the LJ form was replaced by a hydrogen bonding term. Two-color TOFMS has identified two pyrazine configurations, which are depicted in Fig. 1 as **A** and π/2 rotated base pyrazine form of **H**. Besides two-color TOFMS, IR–UV spectroscopy is also helpful technique to be used for the structural identification of gas-phase complexes as performed in the study of Busker et al. [30] for the pyrazine dimer. Moreover, Busker et al. [30] also performed two-color TOFMS experiments, and their results were in agreement with earlier measurements [52] indicating the presence of two pyrazine isomers. Busker et al. [30] found completely different IR–UV double-resonance spectra for these isomers: one could have CH···N interactions and the other one could be a sandwiched, PD or T-shaped orientation. To clarify, especially the structure of second isomer, they performed B3LYP-D and MP2 geometry optimizations and subsequent frequency calculations employing both TZVP and TZVPP basis sets using various pyrazine dimers most of which were shown in Fig. 1. They assigned the first isomer to the planar doubly hydrogen-bonded **A**. For the second isomer, the best agreement between the experimental and calculated IR frequencies was obtained for **B** and **K** orientations, and they assigned the spectrum of the second isomer to the more stable cross-displaced stacked structure **B**. In the current study, **A** and **B** were also located as the most stable pyrazine dimer structures.

Our calculations agreed with Busker et al. [30] and Mishra et al. [29]: B3LYP-D almost reproduces the interaction energies calculated at the CCSD(T) level, and isomer **A** is the lowest energy dimer structure. A similar performance of B3LYP-D has already been shown for the PD orientation of the benzene dimer [53]. However, B3LYP-D underestimates the interaction energies for the sandwich conformer of the benzene dimer and H_2S–benzene dimer at the equilibrium distances. Generally, it tends to overestimate at the short intermolecular separations and slightly underestimate at larger separations. Moreover, it predicts shorter cms distances by 0.1 Å compared to CCSD(T) results [53]. These observations are more or less true for PBE-D and meta-generalized gradient approximation functionals M05-2X and M06-2X [53].

In addition to the results of Busker et al. [30] and Mishra et al. [29], Table 2 indicates that the best agreement with CCSD(T) was obtained with DFT-SAPT(LPBE0AC), which requires similar computer resources like DFT-SAPT(PBE0AC). Even though DFT-SAPT(PBE0AC) reproduces trends observed in CCSD(T), it slightly underestimates the interaction energies. Overall, B3LYP-D seems to be the fastest and accurate enough to compute the potential energy surface (PES) of pyrazine dimer. However, the results shown in Fig. 2 and Table 2 were obtained only for the global minimum structures. Therefore, for a more reliable comparison, the performance of all methods was investigated by computing the interaction energies in various cms distances.

We have selected orientations **A** (hydrogen-bonded), **B** (cross-displaced stacked), **D** (T-shaped: N···π) and **J** (T-shaped: CH···π) to build their potential energy curves (PEC). Only the PEC of **B** was produced using aug-cc-pVDZ basis set due to the lack of symmetry, which was prohibiting CCSD(T) calculations. For the other orientations, we employed aug-cc-pVTZ basis set and calculated the interaction energies at MP2, SCS-MP2, B3LYP-D, DFT-SAPT(PBE0AC), DFT-SAPT(LPBE0AC) and CCSD(T) levels. The corresponding PEC curves were shown in Figs. 3, 4, 5 and 6.

As clear from the Figs. 3, 4, 5 and 6, MP2 overestimates the interaction energy for all the considered orientations. However, at least, MP2 is expected to agree to CCSD(T) for the hydrogen-bonded orientation **A**. Since such a

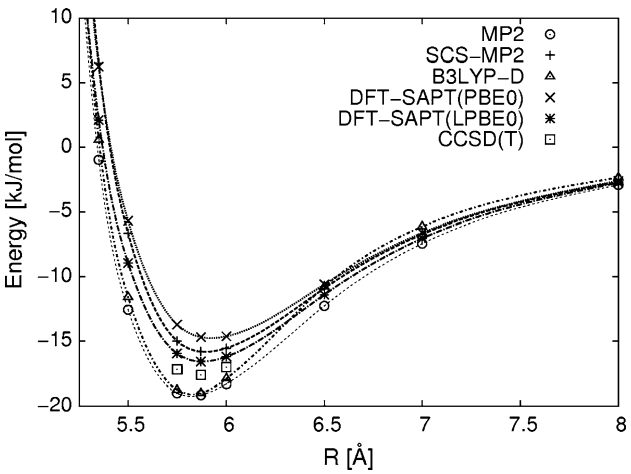

Fig. 3 Potential energy curves obtained from MP2 (*short-dashed*), SCS-MP2 (*long-dashed*), B3LYP-D (*short-dashed* and *dotted*), DFT-SAPT(PBE0AC) (*dotted*), DFT-SAPT(LPBE0AC) (*long-dashed* and *dotted*) and CCSD(T) for orientation **A**

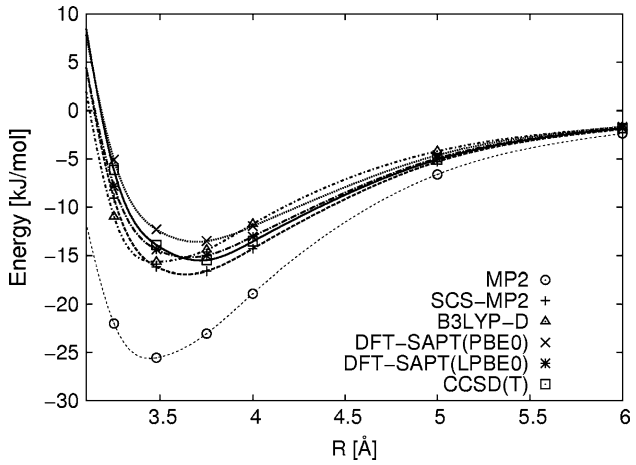

Fig. 4 Potential energy curves obtained from MP2 (*short-dashed*), SCS-MP2 (*long-dashed*), B3LYP-D (*short-dashed* and *dotted*), DFT-SAPT(PBE0AC) (*dotted*), DFT-SAPT(LPBE0AC) (*long-dashed* and *dotted*) and CCSD(T) (*solid*) for orientation B

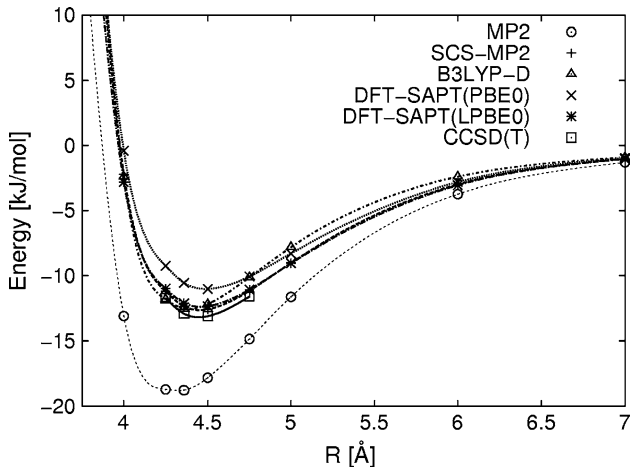

Fig. 5 Potential energy curves obtained from MP2 (*short-dashed*), SCS-MP2 (*long-dashed*), B3LYP-D (*short-dashed* and *dotted*), DFT-SAPT(PBE0AC) (*dotted*), DFT-SAPT(LPBE0AC) (*long-dashed* and *dotted*) and CCSD(T) (*solid*) for orientation D

performance of MP2 was already observed for the hydrogen-bonded acetylene-furan dimer [50], SCS-MP2 corrects MP2 but generally underestimates interaction energies compared to CCSD(T). B3LYP-D fails to treat hydrogen-bonded orientation **A** with an overestimation of the interaction energy similar to MP2 case. Our DFT-SAPT calculations showed that structure **A** is stabilized by both electrostatics and dispersion components. For the other orientations, B3LYP-D slightly overestimates the interaction energies compared to CCSD(T). It seems that the empirical dispersion correction term in B3LYP-D estimates higher dispersion energy. Both MP2 and B3LYP-D performs similar especially at the short range. This, however, is not the case for the long-range part of the PEC's where MP2 still overestimates the interaction energy, whereas B3LYP-

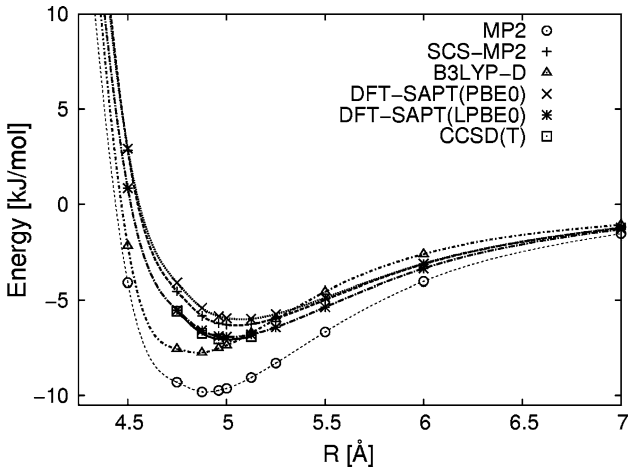

Fig. 6 Potential energy curves obtained from MP2 (*short-dashed*), SCS-MP2 (*long-dashed*), B3LYP-D (*short-dashed* and *dotted*), DFT-SAPT(PBE0AC) (*dotted*), DFT-SAPT(LPBE0AC) (*long-dashed* and *dotted*) and CCSD(T) (*solid*) for orientation J

D starts to underestimation. These features of B3LYP-D were already observed for benzene, H_2S–benzene, methane–benzene and methane dimers [53]. DFT-SAPT(PBE0AC) tends to underestimate the interaction energies more than SCS-MP2 for all the orientations. However, replacing the PBE0AC xc potential with its fully local LPBE0AC variant corrects underestimation behavior of PBE0AC. More importantly, with DFT-SAPT(LPBE0AC), interaction energies become fully agree to CCSD(T) for all the orientations.

In addition to PECs, Table 3 displays the cms distances and interaction energies at their minima employing the aug-cc-pVTZ basis set. Only for orientation **B,** these values were calculated using the aug-cc-pVDZ basis set. It is obvious that MP2 overestimates the interaction energies and underestimates cms distances for all the orientations. SCS-MP2 agrees remarkably well with CCSD(T) especially for the orientations, in which π–π, CH–π and N–π interactions are dominant. Similar to MP2, B3LYP-D estimates the cms minimum distances as shifted to small values for all the orientations. This was also the case appeared in Sherrill et al. [53]. However, it reproduces the corresponding energies in agreement with CCSD(T) except **A**. DFT-SAPT(PBE0AC) tends to overestimate the cms minimum distances for **A** and **J** by 0.08 Å compared to CCSD(T). Clearly, the interaction energies obtained from DFT-SAPT(PBE0AC) were the highest ones in all methods. On the other hand, DFT-SAPT(LPBE0AC) gives the cms minimum distances very close to CCSD(T) ones with a difference of at most 0.03 Å. The minimum energies were also obtained perfectly in agreement with CCSD(T). In particular, it differed from CCSD(T) by 1.04, 0.39, 0.78 and 0.13 kJ/mol for **A**, **B**, **D** and **J**, respectively.

Table 3 Minimum energies [kJ/mol] and cms distances (Å) obtained from MP2, SCS-MP2, B3LYP-D, DFT-SAPT(PBE0AC), DFT-SAPT(LPBE0AC) and CCSD(T) calculations with the aug-cc-pVTZ basis set for A, B, D and J orientations

Isomer	Method	Minimum distance	Minimum energy
A	MP2	5.83	−19.24
	SCS-MP2	5.91	−15.82
	B3LYP-D	5.83	−19.13
	DFT-SAPT(PBE0AC)	5.94	−14.81
	DFT-SAPT(LPBE0AC)	5.86	−16.57
	CCSD(T)	5.86	−17.61
B	MP2	3.45	−25.67
	SCS-MP2	3.66	−16.98
	B3LYP-D	3.47	−15.68
	DFT-SAPT(PBE0AC)	3.70	−13.67
	DFT-SAPT(LPBE0AC)	3.67	−15.27
	CCSD(T)	3.70	−15.67
D	MP2	4.32	−18.87
	SCS-MP2	4.46	−12.65
	B3LYP-D	4.35	−12.53
	DFT-SAPT(PBE0AC)	4.48	−11.04
	DFT-SAPT(LPBE0AC)	4.47	−12.40
	CCSD(T)	4.45	−13.18
J	MP2	4.87	−9.81
	SCS-MP2	5.05	−6.31
	B3LYP-D	4.85	−7.78
	DFT-SAPT(PBE0AC)	5.08	−6.00
	DFT-SAPT(LPBE0AC)	5.00	−6.92
	CCSD(T)	5.01	−7.06

Note that the results for B were obtained using the aug-cc-pVDZ basis set

Table 4 shows the basis set dependence of the interaction energies for all methods at the selected geometries close to the minima of the PECs of **A**, **B**, **D** and **J** orientations. Moreover, this table also includes extrapolated energies using aug-cc-pVTZ and aug-cc-pVQZ results to the CBS limit using the two-point extrapolation method of Bak et al. [54]. Only the second-order dispersion, $E^{(2)}_{\text{disp}}$, and its exchange counterpart, $E^{(2)}_{\text{exch}-\text{disp}}$, were extrapolated in the case of DFT-SAPT. The remaining contributions were taken from the aug-cc-pVQZ results. For MP2 and SCS-MP2, only the electron correlation term (E_{coor}) was extrapolated. In the extrapolation of B3LYP-D energies, the total interactions were used instead of dispersion correction term, which does not depend on the employed basis set. Since performing CCSD(T) calculations with aug-cc-pVQZ basis set is not feasible, a different extrapolation scheme [24] was employed for this case. The difference between the CCSD(T) and SCS-MP2 interaction energies as obtained at the aug-cc-pVTZ level was assumed to be constant, and this difference was added to the extrapolated SCS-MP2 energies to reach to the CBS limit for CCSD(T). Employment of MP2 energies instead of SCS-MP2 hardly changes the extrapolated CCSD(T) energies. As shown in Table 4, MP2 and SCS-MP2 energies for orientation **B** decrease further by 0.9 kJ/mol from triple to quadrupole basis and still decrease by 0.58 kJ/mol from quadrupole to CBS limit. For the other orientations, these differences were obtained to be less dramatic. On the other hand, B3LYP-D seems already converged at the quadrupole level. Even the interaction energy difference between triple and quadrupole zeta basis calculations is not considerably large. DFT-SAPT results reflect a basis set dependence similar to MP2 and SCS-MP2. More specifically, interaction energies were lowered by 0.7 and 0.5 kJ/mol when passing from triple to quadrupole and quadrupole to CBS limit, respectively. Trends in CCSD(T) are much closer to the MP2 and SCS-MP2 cases, for example, for **A,** the CCSD(T) energy was decreased by 0.9 kJ/mol from triple to CBS limit. As a summary, CBS extrapolation does not change the relative performance of MP2, SCS-MP2 and DFT-SAPT methods. However, B3LYP-D becomes more close to the CCSD(T) at the CBS limit. In particular, for **A** and **J,** the absolute difference between B3LYP-D and CCSD(T) energies were calculated to be 1.40 and 0.49 kJ/mol using the aug-cc-pVTZ, respectively. These differences reduced to 0.65 and 0.05 kJ/mol at the CBS limit. It should also be noted that an opposite trend was found for orientation **D**: difference increased from 0.39 to 1.07 kJ/mol.

The most important advantage of DFT-SAPT against supermolecular approach is the ability to split the total interaction energy into individual energy contributions, for example, electrostatics, dispersion and induction. Thus, one can easily determine which forces stabilize the system. Figures 7, 8, 9, 10 display the energy components of DFT-SAPT (PBE0AC) for **A**, **B**, **D** and **J** orientation as a function of cms distances. Among these contributions, $E^{(2)}_{\text{disp}}$, $E^{(2)}_{\text{ind}}$ and $\delta(\text{HF})$ are always attractive, while all the exchange terms are repulsive. $E^{(1)}_{\text{el}}$ is generally attractive, but it can also be repulsive depending on the orientation and cms distance.

For all the pyrazine dimers considered in this study, $E^{(1)}_{\text{el}}$ was obtained to be attractive. The magnitude of the repulsive components displays the following order: $E^{(2)}_{\text{exch}-\text{disp}} < E^{(2)}_{\text{exch}-\text{ind}} < E^{(1)}_{\text{exch}}$. Generally, $E^{(1)}_{\text{exch}}$ covers almost more than half of the total exchange energy. Due to the zero permanent dipole moment of pyrazine, $E^{(2)}_{\text{ind}}$ dies immediately at the short cms distances and $E^{(2)}_{\text{disp}}$ dominates the total interaction at the long range, especially for **B**,

Table 4 Basis set dependence of the interaction energies [kJ/mol] at selected geometries of A (5.87 Å), B (3.48 Å), D (4.36 Å) and J (4.96 Å) using the aug-cc-pVXZ basis sets

Isomer	X	E_{int}					
		MP2	SCS-MP2	B3LYP-D	DFT-SAPT (PBE0AC)	DFT-SAPT (LPBE0AC)	CCSD(T)
A	T	−19.14	−15.81	−19.01	−14.68	−16.57	−17.61
	Q	−19.63	−16.31	−19.08	−14.98	−16.89	–
	CBS	−19.98	−16.67	−19.12	−15.18	−17.10	−18.47
B	T	−27.98	−18.19	−16.18	−14.27	−16.44	–
	Q	−28.87	−19.02	−16.20	−15.00	−17.18	–
	CBS	−29.45	−19.60	−16.22	−15.48	−17.69	–
D	T	−18.78	−12.37	−12.53	−10.56	−12.11	−12.92
	Q	−19.33	−12.87	−12.63	−11.16	−12.74	–
	CBS	−19.67	−13.22	−12.70	−11.55	−13.16	−13.77
J	T	−9.73	−6.21	−7.52	−5.84	−6.88	−7.03
	Q	−10.02	−6.49	−7.54	−6.03	−7.08	–
	CBS	−10.22	−6.69	−7.56	−6.16	−7.22	−7.51

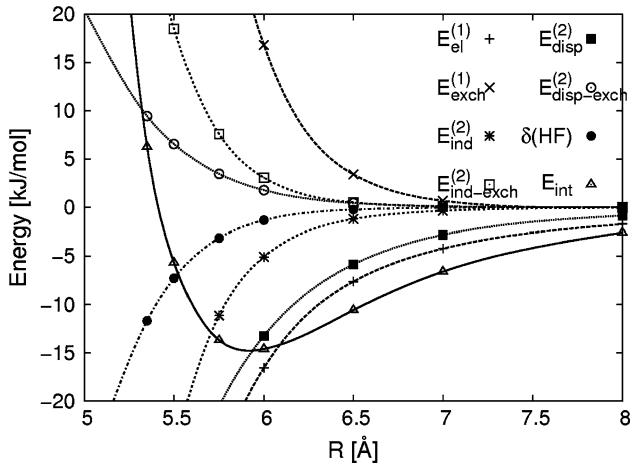

Fig. 7 DFT-SAPT(PBE0AC) energy contributions for the A orientation. *Long-dashed lines* represent $E_{el}^{(1)}$ and $E_{exch}^{(1)}$, *short-dashed* $E_{ind}^{(2)}$ and $E_{exch-ind}^{(2)}$, *dotted* $E_{disp}^{(2)}$ and $E_{exch-disp}^{(2)}$, *dotted long-dashed* δ(HF), and the *solid line* E_{int}

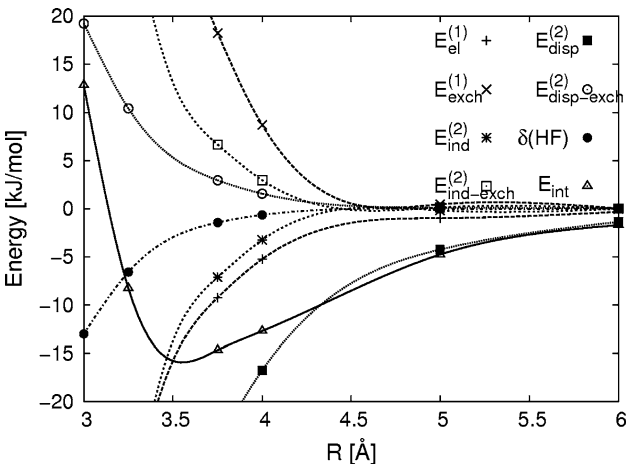

Fig. 8 DFT-SAPT(PBE0AC) energy contributions for the B orientation. *Long-dashed lines* represent $E_{el}^{(1)}$ and $E_{exch}^{(1)}$, *short-dashed* $E_{ind}^{(2)}$ and $E_{exch-ind}^{(2)}$, *dotted* $E_{disp}^{(2)}$ and $E_{exch-disp}^{(2)}$, *dotted long-dashed* δ(HF), and the *solid line* E_{int}

D and **J**. In the case of **A**, $E_{el}^{(1)}$ acts as the major attractive source even at the long range due to the N···H close contacts.

In T-shaped and stacked configurations, $E_{ind}^{(2)}$ plays a significant role by exerting a contribution similar to the electrostatic energy. On the other hand, the induction energy can be seen as diminished by its exchange counterpart as clearly visible from the figures they symmetrically evolves in opposite directions. In contrast, $E_{disp}^{(2)}$ and $E_{exch-disp}^{(2)}$ curves are very different from each other, indicating that the dispersion component is not completely annihilated by its exchange counterpart. Among the considered dimers, the highest dispersion energy was found in the stacked conformation. In particular, the dispersion energy was calculated to be −16.93, −25.16, −22.56 and −14.38 kJ/mol for **A**, **B**, **D** and **J** orientations, respectively, at the equilibrium structures using aug-cc-pVQZ basis set.

Employing the LPBE0AC functional for the xc part in DFT-SAPT calculations lowered the total interaction energies compared to the PBE0AC. This is mostly due to the magnitude of the dispersion contribution in LPBE0AC. In particular, for pyrazine **A** employing aug-cc-pVQZ basis set, $E_{el}^{(1)}$, $E_{ind}^{(2)}$ and $E_{disp}^{(2)}$ components were obtained to be −0.42, −0.88 and −1.64 kJ/mol lower in LPBE0AC compared to PBE0AC. This situation leads to a difference

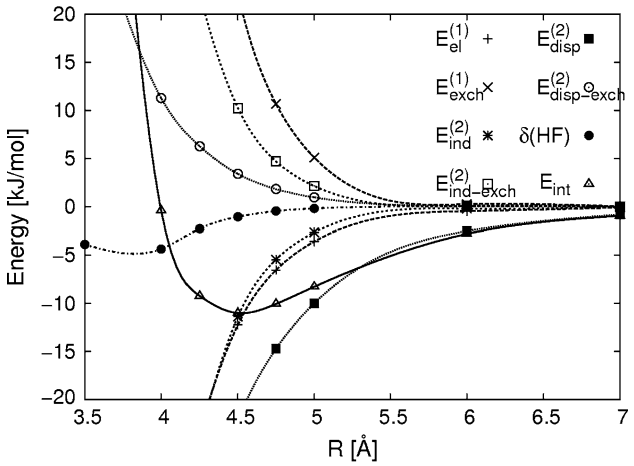

Fig. 9 DFT-SAPT(PBE0AC) energy contributions for the D orientation. *Long-dashed lines* represent $E_{el}^{(1)}$ and $E_{exch}^{(1)}$, *short-dashed* $E_{ind}^{(2)}$ and $E_{exch-ind}^{(2)}$, *dotted* $E_{disp}^{(2)}$ and $E_{exch-disp}^{(2)}$, *dotted long-dashed* δ(HF), and the *solid line* E_{int}

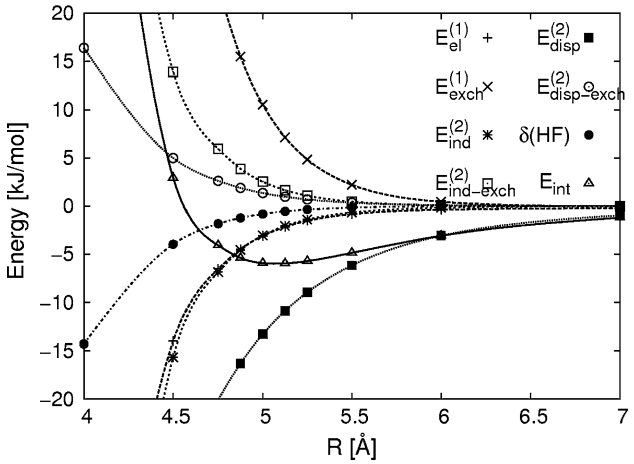

Fig. 10 DFT-SAPT(PBE0AC) energy contributions for the J orientation. *Long-dashed lines* represent $E_{el}^{(1)}$ and $E_{exch}^{(1)}$, *short-dashed* $E_{ind}^{(2)}$ and $E_{exch-ind}^{(2)}$, *dotted* $E_{disp}^{(2)}$ and $E_{exch-disp}^{(2)}$, *dotted long-dashed* δ(HF), and the *solid line* E_{int}

in the total interaction energies around 1.91 kJ/mol. A similar picture was also observed for the other orientations of pyrazine dimer.

3.2 Triazine dimers

To study the intermolecular interactions in 1,3,5-triazine dimer, eight different isomers containing hydrogen-bonded, sandwich, cross-displaced stacked and T-shaped configurations were considered. These structures were illustrated in Fig. 11.

Due to the notable effect of the employed dimer structure in the interaction energy calculations, already shown for pyrizine dimers in Table 1, all 1,3,5-triazine dimers were optimized at the CP-SCS-MP2 level with aug-cc-pVDZ basis set. The corresponding supermolecular and DFT-SAPT interaction energies employing aug-cc-pVDZ basis set were listed in Table 5. Similar to pyrazine case, MP2 and SCS-MP2 yielded the cross-displaced stacked geometry (structure **F** in Fig. 11) as the lowest energy dimer. However, B3LYP-D, DFT-SAPT and CCSD (T) located the doubly hydrogen-bonded structure (structure **A** in Fig. 11) as the most stable isomer.

We also calculated the PECs of the most important four 1,3,5-triazine dimer orientations, namely **A** (hydrogen-bonded), **B** (cross-sandwich), **D** (tilted T-shaped) and **F** (cross-displaced stacked). Here, only for **A**, aug-cc-pVTZ basis set was employed, whereas for the others, aug-cc-pVDZ basis were used due to the lack symmetry, which preventing the corresponding CCSD(T) calculations. In Fig. 12, PECs obtained for orientation **A** were shown. In contrast to pyrazine **A** case, MP2 is quite agree with CCSD(T) results. However, the other methods give almost the similar trends observed for pyrazine **A**.

As shown in Table 6, for **B**, **D** and **F** isomers of 1,3,5-triazine, MP2 overestimates the interaction energy and underestimates the minimum cms distance. Even though B3LYP-D underestimates minimum cms distances, it estimates the interaction energies quite close to CCSD(T) especially for isomer **B**. Generally, SCS-MP2, DFT-SAPT(PBE0AC) and DFT-SAPT(LPBE0AC) correctly reproduce the minimum cms distances in all 1,3,5-triazine dimers. Among these three methods, even though all underestimates the interaction energies, DFT-SAPT(LPBE0AC) seems in a good agreement with CCSD(T).

Similar to pyrazine dimer, DFT-SAPT energy partitioning in 1,3,5-triazine showed that the dispersion and electrostatic contributions are more notable in stacked orientations, for example, **C**, **B**, **F** and **E**, and in CH···N governed orientations, for example, **A**, **G** and **H**. As indicated in Table 5, employment of LPBE0AC functional instead of PBE0AC in DFT-SAPT calculations has resulted to obtain lower interaction energies by at most 1.8 kJ/mol.

A, **D**, **E** and **F** triazine structures resemble to **A**, **C**, **F** and **B** pyrazine isomers, respectively, and thus, one should expect similar interaction energies. This is really the case, for example, **A** and **F** pyrazine conformers were lower in energy than the corresponding triazine dimers by at most 3.71 kJ/mol at all levels of theory employing aug-cc-pVDZ basis set. However, triazine **D** and **F** were obtained lower in energy than the corresponding **C** and **B** pyrazine at the CCSD(T) by at most 2.07 kJ/mol and B3LYP-D but higher at the MP2 and SCS-MP2 levels. Moreover, DFT-SAPT(PBE0AC) favored triazine **D** over pyrazine **C** by 0.52 kJ/mol and pyrazine **B** over triazine **F** by 0.87 kJ/mol. Among the triazine conformers, as

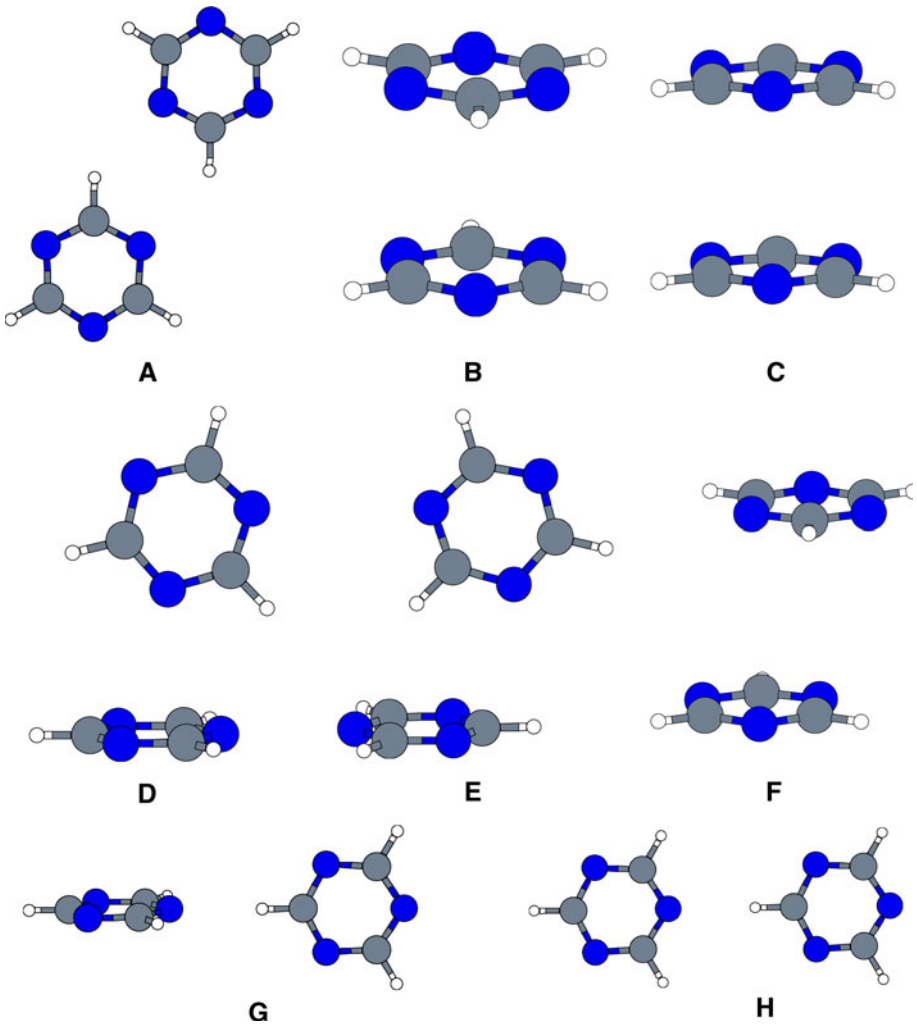

Fig. 11 1,3,5-Triazine dimer orientations considered in this study

Table 5 Calculated interaction energies (E_{int}) [in kJ/mol] at MP2, SCS-MP2, B3LYP-D, DFT-SAPT (PBE0AC), DFT-SAPT (LPBE0AC) and CCSD(T) levels using aug-cc-pVDZ basis set for all triazine orientations, which have been optimized at the CP-SCS-MP2 level employing aug-cc-pVDZ basis set

Isomer	E_{int}					
	MP2	SCS-MP2	B3LYP-D	DFT-SAPT (PBE0AC)	DFT-SAPT (LPBE0AC)	CCSD(T)
A	−15.27	−12.92	−17.89	−13.37	−14.73	−15.53
B	−18.98	−12.78	−14.67	−12.37	−14.03	−14.52
C	−10.66	−4.85	−3.91	−2.75	−4.21	−4.74
D	−15.73	−10.90	−13.31	−9.81	−10.64	−14.23
E	−9.78	−6.14	−9.28	−5.84	−7.03	−7.94
F	−21.09	−13.34	−15.71	−11.45	−13.16	−14.33
G	−8.57	−7.12	−9.89	−7.46	−8.33	−8.68
H	−9.95	−8.47	−11.42	−8.91	−9.82	−10.20

shown in Table 5, **B** (cross-sandwich) was lower in energy than **C** (sandwich) by 9.78 kJ/mol. Recent calculations on the sandwich benzene performed by Sherrill et al. [53] shown that this isomer has a binding energy of 5.56 kJ/mol at the CCSD(T)/aug-cc-pVDZ level. Certainly, the sandwich benzene is more stable than triazine **C** by 0.82 kJ/mol, but triazine **B** has almost three times stronger interaction than the sandwich benzene.

It is also interesting to compare the magnitude of interaction energies in two and three nitrogen-containing

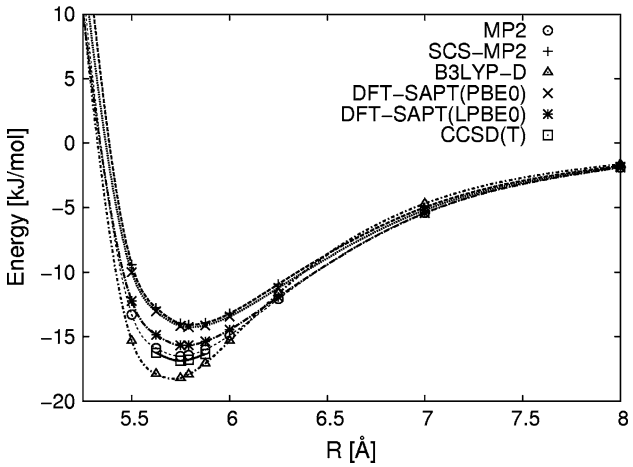

Fig. 12 Potential energy curves obtained from MP2 (*short-dashed*), SCS-MP2 (*long-dashed*), B3LYP-D (*short-dashed* and *dotted*), DFT-SAPT(PBE0AC) (dotted), DFT-SAPT(LPBE0AC) (*long-dashed* and *dotted*) and CCSD(T) (*solid*) for orientation A

Table 6 Minimum energies [kJ/mol] and cms distances (Å) obtained from MP2, SCS-MP2, B3LYP-D, DFT-SAPT(PBE0AC), DFT-SAPT(LPBE0AC) and CCSD(T) calculations with the aug-cc-pVTZ basis set for **A** and aug-cc-pVDZ basis set for **B**, **D** and **F** orientations

Isomer	Method	Minimum distance	Minimum energy
A	MP2	5.74	−16.51
	SCS-MP2	5.79	−14.06
	B3LYP-D	5.72	−18.27
	DFT-SAPT(PBE0AC)	5.79	−14.25
	DFT-SAPT(LPBE0AC)	5.77	−15.68
	CCSD(T)	5.76	−16.88
B	MP2	3.42	−19.01
	SCS-MP2	3.50	−13.23
	B3LYP-D	3.39	−14.75
	DFT-SAPT(PBE0AC)	3.49	−12.65
	DFT-SAPT(LPBE0AC)	3.48	−14.15
	CCSD(T)	3.49	−14.72
D	MP2	4.40	−15.74
	SCS-MP2	4.48	−11.20
	B3LYP-D	4.40	−13.34
	DFT-SAPT(PBE0AC)	4.49	−10.17
	DFT-SAPT(LPBE0AC)	4.47	−11.32
	CCSD(T)	4.46	−14.31
F	MP2	3.43	−21.09
	SCS-MP2	3.50	−13.84
	B3LYP-D	3.43	−15.72
	DFT-SAPT(PBE0AC)	3.61	−12.17
	DFT-SAPT(LPBE0AC)	3.50	−13.61
	CCSD(T)	3.50	−14.78

aromatic rings with one nitrogen-containing pyridine dimers. In the recent study of Mishra et al. [29], cross-displaced stacked and doubly hydrogen-bonded orientations of pyridine were also investigated. For the most stable cross-displaced stacked conformer of pyridine, a binding energy of 10.12, 13.89 and 25.40 kJ/mol was obtained employing CCSD(T)/aug-cc-pVDZ, B3LYP-D/aug-cc-pVTZ and MP2/CBS levels, respectively. Apparently, these energies were slightly higher than pyrazine **B** by 3.78, 2.29 and 4.05 kJ/mol at the corresponding levels. In the case of the hydrogen-bonded orientation, intermolecular interactions obtained for pyrazine **A** was found to be lower by 1.13 and 1.15 at CCSD(T)/aug-cc-pVDZ and MP2/CBS, respectively. However, B3LYP-D/aug-cc-pVTZ results of Mishra et al. [29] showed that the hydrogen-bonded pyridine and pyrazine **A** are isoenergetic. Besides pyridine and pyrazine, Mishra et al. [29] also studied several triazine dimers including cross-displaced stacked **F** and doubly hydrogen-bonded **A**. Similar to the current study, their estimated CCSD(T)/CBS results indicated that structure **A** is more stable than **F** by 0.46 kJ/mol. Furthermore, binding energies obtained in the current study for triazine **F** was lower in energy in comparison with Mishra et al. [29] by 0.55 and 1.49 kJ/mol at the MP2/aug-cc-pVDZ and CCSD(T)/aug-cc-pVDZ levels, respectively. A similar trend was observed for triazine **A** with approximately 0.5 kJ/mol lowered interaction energies. Since Mishra et al. [29] did not employ the CP correction to the dimer geometries, their corresponding interaction energies should be slightly lowered if the CP correction is enabled. This trend was already shown in Table 1 for pyrazine. Apparently, for the similar dimer structures of pyridine, pyrazine and triazine, the resulting intermolecular interactions are very close to each other and which are notably lower in energy than the corresponding benzene dimers.

4 Conclusions

Weak intermolecular interactions in dimers of nitrogen-containing heteroaromatic compounds such as pyrazine and 1,3,5-triazine were investigated accurately by CP-corrected supermolecular MP2, SCS-MP2, B3LYP-D and CCSD(T) and DFT-SAPT (PBE0AC and LPBE0AC) methods. We showed that instead of MP2-optimized geometries, starting with CP-SCS-MP2-optimized geometries causes the interaction energies to be lowered by 1–2 kJ/mol. In both dimer systems, similar local minimum structures were found. Among them, doubly hydrogen-bonded isomer was obtained to be the most stable isomer. However, both of MP2 and SCS-MP2 favored the stacked **B** and cross-displaced stacked **F** isomers for pyrazine and 1,3,5-triazine, respectively. Even though B3LYP-D

resulted in very close interaction energies with CCSD(T) at the equilibrium geometries, it tends to overestimate at the short intermonomer separations and underestimate at the long range. Moreover, it gives smaller equilibrium distances compared to CCSD(T). These handicaps of B3LYP-D limit its usage to calculate the PES of these dimers. DFT-SAPT(PBE0AC) and DFT-SAPT(LPBE0AC) produced as similar energy ordering as CCSD(T), especially for the pyrazine dimer. In the case of 1,3,5-triazine, the best agreement with CCSD(T) energy orderings was obtained when DFT-SAPT(PBE0AC) and DFT-SAPT(LPBE0AC) methods have been employed. Since DFT-SAPT method produces comparable results to CCSD(T) results, and it is less expensive than coupled cluster methods, it enables to produce the full PES of these dimers. Furthermore, these methods seem to be the best candidates to investigate the structures of nucleic acid bases and other systems stabilized by π–π and CH···N interactions.

Acknowledgments Computing resources used in this work were provided by the National Center for High Performance Computing of Turkey (UYBHM) under grant number 20662009 and Informatics Institute of Istanbul Technical University.

References

1. Broda M, Siodlak D, Rzeszotarska B (2005) J Peptide Sci 11:235
2. Stojonovic S, Medokovic V (2007) J Biol Inorg Chem 12:1063
3. Börnsen KO, Selzle HL, Schlag W (1986) J Chem Phys 85:1726
4. Grover JR, Walters EA, Hui ET (1987) J Chem Phys 91:3233
5. Krause H, Ernstberger B, Neusser HJ (1991) 184: 411
6. Arunan E, Gutowsky HS (1992) J Chem Phys 98:4294
7. Hobza P, Selzle HL, Schlag EW (1993) J Phys Chem 97:3937
8. Hobza P, Selzle HL, Schlag EW (1994) J Am Chem Soc 116:3500
9. Tsuzuki S, Uchimaru T, Mikami M, Tanabe K (1996) Chem Phys Lett 252:206
10. Hobza P, Selzle HL, Sclag EW (1996) J Phys Chem 100:18790
11. Jaffe RL, Smith GD (1996) J Chem Phys 105:2780
12. Špirko V, Engkvist O, Soldán P, Selzle HL, Schlag EW (1999) J Chem Phys 111:572
13. Tsuzuki S, Uchimaru T, Matsumura K, Mikami M, Tanabe K (2000) Chem Phys Lett 319:547
14. Tsuzuki S, Honda K, Uchimaru T, Mikami M, Tanabe K (2002) J Am Chem Soc 124:104
15. Sinnokrot MO, Valeev EF, Sherril CD (2002) J Am Chem Soc 124:10887
16. Sinnokrot MO, Sherril CD (2004) J Phys Chem A 108:10200
17. Sinnokrot MO, Sherril CD (2004) J Am Chem Soc 126:7690
18. Tauer TP, Sherrill CD (2005) J Phys Chem A 109:10475
19. Haßelmann A, Jansen G, Schütz M (2005) J Chem Phys 122:014103
20. Sinnokrot MO, Sherril CD (2006) J Phys Chem A 110:10656
21. Podeszwa R, Bukowski R, Szalewicz K (2006) J Phys Chem A 110:10345
22. Hill JG, Platts JA, Werner HJ (2006) Phys Chem Chem Phys 8:4072
23. Lee EC, Kim D, Jurečka P, Tarakeshwar P, Hobza P, Kim KS (2007) J Phys Chem A 111:3446
24. Janowski T, Pulay P (2007) Chem Phys Lett 447:27
25. Gräfenstein J, Cremer D (2009) J Chem Phys 130:124105
26. Mishra BK, Sathyamurthy N (2005) J Phys Chem A 109:6
27. Piacenza M, Grimme S (2005) Chem Phys Chem 6:1554
28. Mishra BK, Sathyamurthy N (2006) J Theor Comput Chem 5:609
29. Mishra BK, Arey JS, Sathyamurthy N (2010) J Phys Chem A 114:9606
30. Busker M, Svartsov YN, Häber T, Kleinermanns K (2009) Chem Phys Lett 467:255
31. Wang W, Hobza P (2008) Chem Phys Chem 9:1003
32. Wang W, Hobza P (2006) Chin J Chem Phys 19:401
33. Guin M, Patwari GN, Karthikeyan S, Kim KS (2009) Phys Chem Chem Phys 11:11207
34. Ahlrichs R, Bär M, Häser M, Horn H, Kölmel C (1989) Chem Phys Lett 162:165
35. Grimme S (2003) J Chem Phys 118:9095
36. Grimme S (2004) J Comput Chem 25:1463
37. Grimme S (2006) J Comput Chem 27:1787
38. Jeziorski B, Moszynski R, Szalewicz K (1994) Chem Rev 94:1887
39. Szalewicz K, Patkowski K, Jeziorski B (2005) Struct Bonding 116:43
40. Jansen G, Haßelmann A (2001) J Phys Chem A 105:11156
41. Haßelmann A, Jansen G (2002) Chem Phys Lett 357:464
42. Haßelmann A, Jansen G (2002) Chem Phys Lett 362:319
43. Haßelmann A, Jansen G (2003) Chem Phys Lett 367:778
44. Misquitta AJ, Podeszwa R, Jeziorski B, Szalewicz K (2005) J Chem Phys 123:214103
45. Werner HJ, Knowles PJ, Lindh R, Manby FR, Schütz M, Celani P, Korona T, Rauhut G, Amos RD, Bernhardsson A, Berning A, Cooper DL, Deegan MJO, Dobbyn AJ, Eckert F, Hampel C, Hetzer G, Lloyd AW, McNicholas SJ, Meyer W, Mura ME, Nicklass A, Palmieri P, Pitzer R, Schumann U, Stoll H, Stone AJ, Tarroni R, Thorsteinsson T MOLPRO, version 2009.1, a package of ab initio programs, see http://www.molpro.net
46. Weigend F (2002) Phys Chem Chem Phys 4:4285
47. Weigend F, Köhn A, Hättig C (2002) J Chem Phys 110:3175
48. Lias SG Ionization energy evaluation, in NIST chemistry webbook. In: Linstrom PJ, Mallard WG (eds) NIST standard reference database number 69, June 2005. National Institute of Standards and Technology, Gaithersburg, MD, 20899, (http://webbook.nist.gov)
49. Tekin A, Jansen G (2007) Phys Chem Chem Phys 9:1680
50. Sanchez E, Mardyukov A, Tekin A, Crespo-Otero R, Montero LA, Sander W, Jansen G (2008) Chem Phys 343:168
51. Wanna J, Bernstein ER (1986) J Chem Phys 85:3243
52. Wanna J, Menapace JA, Bernstein ER (1986) J Chem Phys 85:777
53. Sherrill CD, Takatani T, Hohenstein EG (2009) J Phys Chem A 113:10146
54. Bak KL, Jørgensen P, Olsen J, Helgaker T, Klopper W (2000) J Chem Phys 112:9229